Tests of the MVD beam test electronics with the laser station

John P. Sullivan and Hubert W. van Hecke
Los Alamos National Laboratory, Los Alamos, NM 87544

February 10, 1997

PHENIX-MVD-97-1

Abstract

Tests of the MVD beam-test electronics system have been done using an infrared laser (1064 nm) system coupled to a stepping motor. The electronics system is read out using the same computer and software as was used in the beam test in spring 1996. The computer also controls the movement of the stepping motor which moves the laser. The diameter of the laser spot is about 50 μm and the stepping motor can position it to within about 10 μm. All channels of the system were tested with the laser, with some channels selected for more detailed tests. We were not able to improve the signal to noise measurement beyond the results from the beam test. We noticed that the channel numbering is not trivially related to the position of the channel on the detector.

1 Introduction

Silicon detectors can be tested using a 1064 nm infrared diode laser. A station to do this was constructed by Shaheen *et al.* in Los Alamos[1]. The hardware described by Shaheen *et al.* was used in these tests. The laser system consists of the following:

- a 1064 nm IR laser diode which sits on a small circuit board containing trigger and monitoring circuitry,
- an externally triggered pulser which triggers the laser,
- a fiber optic cable with a lens at the end which transmits the light from the diode to the Si strip detector and focuses it,
- a stepping motor which can move the laser in 10 μm steps in either "x" (transverse to the strip direction) or "y" (along the strip direction),
- a camac/GPIB interface to control the stepping motor,

- software running on an hp-735 (unix based) computer which controls the stepping motor through the camac/GPIB interface

The last two items in this list were not part of the system used by Shaheen *et al.*. The interface used to control the stepping motor and the associated software replaced MacIntosh-based software which was used to control the stepping motor in the past. This change was made because the MVD beam test electronics are read out via a CODA-based acquisition system running on an hp-735 computer. The tests described here are impractical when one computer controls the stepping motor and another reads the electronics.

The MVD beam test electronics were developed by the Oak Ridge Group. The system was tested in the beam at BNL in Spring 1996. Some details of this test can be found on the WWW[2]. The tests described in this document used the same MVD beam test electronics system, but they did not include either the cooling system or the external noise shields used in that test. The system was enclosed in a steel box to shield the electronics from external light.

2 Some details on the setup and analysis

The readout of the electronics is done using a CODA (Cebaf Online Data Acquisition) system. The same acquisition software was used in the beam test, except that a few small changes were made for these tests described here. The most significant difference was adding code to move the stepper motor (which controls the position of the laser) and to read back the current position of the stepper motor.

Some of the problems encountered in these tests were caused by a large amount of electronic noise picked up by the MVD beam test electronics when the stepper motor was powered on. This could be seen both in the digital readout and (on the scope) in the the preamp spy channel outputs. It amounted to several hundred millivolts of noise on the preamp output – much larger than the typical 80 mV signal expected for a minimum ionizing particle (mip). For this reason, some of the tests (see section 4) were done by moving the laser onto the strip being tested (with the stepper motor) and then turning the stepper motor off to reduce the overall level of noise.

Not only did the noise from the stepper motor significantly reduce the signal to noise in the system, it also strongly interfered with the digital aparatus in the FEE. The interference manifested itself in that words were dropped from apparently random positions in the event packets received by the data acquisition system. The ADC's used in the system were 11 bits, which means a maximum digitized value of 2047. The data format also included header and trailer words for each event. All events were checked for proper format in the readout – if any of the ADC values was outside the range 0-2047, or if the header and/or trailer words were not correct, the entire event was rejected. The ADC values have no address encoded with them, so when the wrong number of values is seen, there is no reasonable alternative to rejecting the whole event. When the stepper motor was powered on, from 50 to 70% of the events failed this test – indicating an error in data transmission. This error rarely occurred when the stepper motor was off. We do not know exactly why, how, or where in the system this failure occurs. It could be in the

MVD electronics or in the readout electronics or software. In some of the tests described below, the fraction of all events which have the correct format is called the "efficiency".

Each "event" in the readout system contained the "pre-sample" ADC value (from the clock cycle prior to the trigger) and the "post-sample" ADC value (from the clock cycle after the trigger) for each of the 64 channels of instrumented electronics. In the discussion which follows, the "single-difference" ADC value is the difference between the post-sample ADC and the pre-sample ADC. During the beam test, a correlation in the noise between different channels in the same group of 8 (which share the same pre-amp, etc) was noticed. In other words, if one channel in a group of 8 channels fluctuated upwards, the others in the group seemed to fluctuate in the same direction. The "single-difference" distributions should correct for fluctuations slow compared to the clock (400 ns), but higher frequency fluctuations will not be corrected. The "double-difference" was introduced in the beam test as a solution to this problem. In each group of 8 channels, the one channel with the largest ADC signal is determined. Then, the average value of the "single-difference" is found for the other 7 channels in the group of 8. This average "single-difference" is used as a correction for all channels in the group of 8. This correction is based on the assumption that the real signal appears in only one channel. The algorithm is reasonable for the tests described here. However, in the real Phenix experiment many of the channels will be hit in any group of channels – so this assumption is not valid and it is unlikely that this noise reduction from the "double-difference" will be possible.

Because the current position of the stepper motor is reset to x=y=0 whenever the stepper motor is turned off, the values of "x" and "y" can have different origins in different tests. The stepper motor can be moved in steps as small as 10 μm. In the tests described here, the laser was moved to approximately the middle of the strips (in "y", the direction along the strips) and remained at the same "y" position throughout the tests. The laser was moved in "x" to test the response of the various strips, where "x" is the direction transverse to the strip direction.

3 Results of scans across the detector wafers

In all of the scans described in this section, the laser bias was 34 Volts, which corresponds to roughly 7 "mips". The Silicon bias was set at 30 Volts.

One series of tests consisted of scanning the laser across the strips (the "x" direction) and reading out all channels at each of the x positions. Figures 1 – 4 show scans across channels 1-16, 17-32, 33-48, and 49-64, respectively. Channels 1-32 are on the first of the two detector wafers and channels 33-64 are on a second detector wafer. Each scan was done by moving the laser in steps of 20 μm. At each point all 64 channels were read out 30 times (pre-sample and post-sample). Although all 64 channels were read, each scan was only over one of the two detector wafers (32 channels). Each of the plots (figures 1 – 4) shows the mean "double-difference" ADC value for a given channel for the laser position shown on the horizontal axis. Although the scan used 20 μm steps, figures 1 – 4 use 80 μm bins in laser position. The error bars show the rms deviation of all measurements in the bin from the mean – so the size of the error bars is a measure of the noise in the channel – smaller is better. These distributions should be centered at zero when the laser is not pointed at the channel and should show a peak when the laser is pointed at the channel. Since the laser position bins are 80 μm wide, the strips are 200 μm wide, and the laser spot is about 50 μ wide, the peak should be around 3 bins wide.

Looking at figures 1 – 2, which show the scans for channels 1-16 and 17-32, respectively, there are never any clear peaks. There are hints of a small response in channel 16 around +0.5 mm, and in channels 30-32 around -3 mm. It is not clear why these channels were not working when the scans were done. These results are shown only for completeness – all other tests were done on channels 33-64. One effect that can be seen (for example in ch. 4) is that the noise seems time dependent. An entire scan takes about 20 minutes, and in some channels the noise changes by a sizable factor over this time period. In this particular example time increases as x increases in the plots – which means that the noise appeared to decrease with time. More typically, we found that noise increased with time. Eventually, typically 5 or 6 hours after everything was turned on, the noise reached became so large that all ADC values were always overflowed and the system could not be used. Turning the system off overnight cured this problem. Tunring in off for a few minutes did not usually help. We interpret this as a cooling problem somewhere in the system. We are not sure whether the problem was in the MVD electronics or in the readout system (VME or camac modules for example). Remember that the cooling system for the MVD electronics system was not used in these tests.

Figures 3 – 4 show the scans over channels 33-64. For this detector, most of the instrumented channels were working – as seen by the narrow peaks in the distributions. From figure 3 we can see that channels 34, 35, 39, 40, and 42 were not working while channels 33, 36-38, 41, 43-48 were working. From the widths of the distributions when the laser was not pointed at the channels, we can see that the first 8 channels are generally noisier than the second 8. From figure 4 we can see that channels 49-64 were all working and that channels 53 and 57 are somewhat noisier than the others.

In figure 5 a laser scan in the vicinity of a single "working" strip is shown in greater detail. This plot uses the same data as was used to generate the corresponding plot for channel 61 in figure 4, but this time the data are plotted in 20 μm bins (rather than 80 μm). In addition the scale is expanded to show only the region close to the strip. This plot shows the characteristic double-peaked structure which is seen in laser scans of these strip detectors. There is a 50 μ wide aluminum strip (used to read the charge on the strip) at the center of each Si strip. The laser's light is reflected by the aluminum and therefore does not penetrate the silicon. Therefore, little or no signal is seen when the laser shines directly on the center of the strip. Each strip is 200 μ wide, and a signal is seen when the laser is moved to either side of the aluminum strip, but the signal rapidly vanishes when the laser is moved more than 100 μm from the center of the strip. From this plot, we can also see that there is not much cross talk in the MVD beam test electronics system. At the precision of these measurements, channel 61 shows no response when the laser is pointed to channel 60 (which is centered at an x value 200 μm or 0.2 mm below strip 61) or channel 62 (which is 0.2 mm higher in x).

The scans shown in figures 1 – 5 can also be used to estimate the relative gains of all channels[3]. Figure 6 summarizes the technique. The left side of the plot shows some of the same laser scan data as are shown in figure 4, for channels 53-56. The pair of vertical lines are calculated from the laser position, and predict where the signal should show up. In this plot, the width of the window is 200 μm (the width of a strip). On the right side of the plot, "double difference" ADC distributions are shown for the individual channels. The top plot of each pair shows the ADC distribution over the entire scan. The bottom plot of each pair shows the ADC distribution inside the narrow "signal window" marked on the plot to the left. To this signal, a gaussian was fit, excluding counts less than zero. The cut fishes out the signal for the four shown channels. Channel 53 is noisier than 54-56. This is clear in the width of the baseline in the left plots and in the signal distribution on the top right. These channels serve as an example of the technique. More details for other channels can be found in reference [3].

Using the technique summarized in figure 6, a summary plot (figure 7) was constructed showing the mean signal height as a function of channel number. These are the means of the gaussians fit to the signals fished out of the scan plots. Dead channels show up at -99. The signal for non-dead channels is around 330, but falls to 220 across the 3rd chip, and in the 4th chip rises from 140 to 260. Further details are given in reference [3].

The data from the scans was also used to generate the two-dimensional plot shown in figure 8. The horizontal axis shows the strip number and the vertical axis shows the laser position. The size of the boxes is proportional to the number of channels with the double-difference ADC value for the channel greater than 200. Dotted horizontal and vertical lines indicate the divisions between groups of 8 channels which share the same pre-amp chip. Four diagonal lines are clearly visible. These diagonal lines show that the channel numbers are not trivially related to the x position on the detector. Essentially, when moving across a detector, the pre-amp numbers increase in one direction and the channels numbers within a pre-amp increase in the other direction. If there is so obvious geometric problem in the layout of the electronics which requires this complicated relationship between channel number and position, we would like to see in changed in future versions of the electronics.

4 Tests of selected individual channels

The laser scans shown in the previous section test all of the channels in the system. A few channels were selected for more detailed tests. In these more detailed tests, the laser was moved to point to the strip being tested and remained in the same position throughout the tests of that strip. Four measurements were made for each of the channels:

- an ADC distribution with the **laser off** and the **stepper motor off**,
- an ADC distribution with the **laser on** and the **stepper motor off**,
- an ADC distribution with the **laser off** and the **stepper motor on**,
- an ADC distribution with the **laser on** and the **stepper motor on**.

Among the channels which were selected for these more detailed tests were two channels which did not appear to be working in the laser scans (channels 34 and 35) and three channels which did appear to be working in in the laser station scans (channels 36, 54, and 61). Of these, channel 54 is of particular interest because it was used to estimate the signal to noise in the beam test measurements. The relative gains of the different channels should be taken from figure 8. The relative gains of the different channels in figures 9 – 18 depends on details of the positioning of the laser. As can be seen from figure 5, the output amplitude depends on the exact position of the laser – since no effort was made to perfectly position the laser, the relative amplitudes from different channels can not be quantitatively compared.

The results of these tests are shown in figures 9 – 18. Each of the figures has ADC distributions for the four conditions tests (laser on/off, stepper motor on/off). For each channel one figure shows the "single difference" ADC distribution and another figure shows the "double difference" distribution. The mean of the ADC distribution and the rms width of the distribution is shown on each plot. In addition, the "efficiency" is shown for condition. The "efficiency" is the fraction of events which appear valid – see section 2 for further details. When comparing to the beam test results, the distributions with the stepper motor off (the top two on each plot) are most relevant – the stepper motor is an external source of noise which was not present in the beam test and will not be present in Phenix. Here, we will assume that no similarly horrible noise source will exist in Phenix. The bottom two plots on each figure show the results with the stepper motor on and give us some understanding of the level of additional noise which is present in the laser scans (which require the stepper motor to be on). The left side of each plot shows the ADC distribution with the laser off – the pedestal value (which should be centered at zero) and width is determined from these plots. The right side of each figure shows the ADC distributions with the laser on. The laser had a bias voltage of about 34V, corresponding to roughly a 7 "mip" signal. The bottom plots, with the stepper on, usually show much wider ADC distributions (larger rms), but the peaks appear at about the same ADC value.

Figures 9 and 10 show the "single" and "double-difference" ADC distributions for channel 34. This was a channel which was not working during the laser scans and was also one of the noisier channels tested. The more detailed information shown in these plots is consistent with the initial diagnosis – turning the laser on does not appear to significantly change the ADC distribution. In addition, the channel appears to be very noisy, with or without the stepper motor being turned on. This channel has an unusual characteristic – the "single-difference" ADC distribution is wider (noisier) with the stepper motor off. The problem behavior reverses when using the double difference – the distributions with the stepper motor off are narrower than with the motor on. The additional strange feature of this channel is that the double difference distributions are wider than the single differences when the stepper motor is on. The double difference is not helping this channel, apparently some of the fluctuations in the signal of this (apparently dead) channel are not related to the adjacent channels.

Figures 11 and 12 show the "single" and "double-difference" ADC distributions for channel 35. This was another relatively noisy and apparently dead channel during the laser scans. Again the results are consistent with the laser scan – there is no apparent response to the laser and the channel is relatively noisy. For this channel, the distributions with the stepper motor are always wider (noisier) than with the stepper motor on. For this channel the double difference distributions are wider than the single difference distributions whether or not the stepper motor is on. As with channel 34, the fluctuations in the ADC values from channel 35 do not seem to be related to the ADC values for the other channels in its group of 8 – so the double difference method makes it worse instead of better.

Figures 13 and 14 show the "single" and "double-difference" ADC distributions for channel 36. Based on the scans, channel 36 was a relatively noisy, but working channel. The more detailed examination is consistent with scan. When the stepper motor is on (as in the laser scan) the pedestal is relatively wide. The channel does respond to the laser – there is a clear difference between the left and right sides of the plots. The double difference distributions are about 40 % narrower than the single difference distributions when the stepper motor is off. The level of noise in the double difference distributions may be affected by using channel 34 and 35 (which were nor working) in calculating the double-difference for this channel. The fluctuations (which are usually small) in channels 34 and 35 are used in calculating the double difference for channel 36, but their fluctuations do not seem to be correlated. The laser off, stepper motor off results for channel 36 show one other unusual feature – it is the only case for which the "efficiency" with the stepper motor off is not close to 100%. This is not really as atypical as the results shown in this note suggest – the system tends slowly stop working with time. In general, the longer it remains powered up, the greater the probability of bad events. This is true whether or not the stepper motor is on. We interpret this as a cooling problem either in the (uncooled in these tests) MVD electronics or in the readout hardware we use.

Figures 15 and 16 show the "single" and "double-difference" ADC distributions for channel 54. Based on the laser scans, channel 54 was one of the better channels. It is also the channel which was used for the most the detailed analysis of the data taken in the Spring 1996 beam test[2]. The single difference distributions from channel 54 show a double-peaked pedestal when the stepper motor is off. There is a clear response to the laser. The mean signal with the laser on is about 420 ADC channels (from the double-difference distribution with the stepper motor off). In the beam test, the mean signal for a particle hitting this channels was about 60 ADC channels. From these two numbers, the number of "mips" equivalent of the laser signal used in these tests is $\approx 420/60 = 7$ mips. When the stepper motor is on, the distributions are significantly wider. The double difference distributions are narrower than the single difference distributions. The peak in the double difference ADC distribution has a shoulder at slightly lower ADC values. The shoulder is probably caused by a timing problem in the level-1 trigger to the system. The pulsing of the laser is not synchronized with the clocks on the electronics boards. We attempted to optimize the delay of the level-1 trigger, but it is not perfect and sometimes the pre- or post-sample comes on the rising edge of the analog output rather than coming before and after the rise in the pre-amp output. This problem could be fixed with a more sophisticated trigger circuit (which used the clocks) but this was not done in these tests.

Figures 17 and 18 show the "single" and "double-difference" ADC distributions for channel 61. Based on the laser scans, channel 61 was one of the better channels. In these tests it is similar to channel 54.

5 Comparison to the beam test results

The signal to noise estimate from the Spring 1996 beam test [2] said that the one "mip" signal appeared in about channel 60 and the pedestal width (sigma) was about 10 channels. This was done for channel 54. This gave a signal to noise ratio of $60/10 = 6/1$. The number of ADC channels equivalent to one "mip" must come from the beam test of this channels – the laser station can not give us a more reliable number. If we could get a narrower pedestal value working on the laser station, we could reasonably assume that the same performance would be seen in any future beam test. The narrower pedestal would then translate directly into an improvement in the signal to noise. This would not really be a test related to the laser (since we get the pedestal without the laser), but it could be done with this system. So far, the best performance for channel 54 seen on the laser station is shown in figure 16 – where the pedestal sigma is 14 channels when the stepper motor is off. This is worse than in the beam test. Perhaps some improvements in the system (grounding, shielding, cooling, ... ?) could reduce this width, but we have been unable to do better so far.

6 Conclusions

The results from the tests of the MVD beam test electronics have shown us the variation in ADC response for the same input signal (from the laser). In figure 7, the ADC values varied from about 140 to 330 ADC channels for the same input. We have also seen that the laser station can find bad channels and can characterize the performance of both good and bad channels. The system has more noise in it than was seen in the beam tests. We are still investigating this problem. However, the results to date do not allow us to assume that the signal to noise in this system is any better than was seen in the Spring 1996 beam test. Based on the two bad channels which were tested in detail (section 4), it seems that the double-difference correction for correlated fluctuations in groups of 8 adjacent channels does not work for bad channels – their fluctuations are not correlated with those of their neighbors. finally, the channel number are not numbered consecutively across the detector – the authors of this report hope that will change in the final system.

References

[1] S. Shaheen, J. Boissevain, W. Collier, B. V. Jacak, J. S. Lock, P. Roybal, J. Simon-Gillo, W. Sondheim, J. P. Sullivan, and H. Ziock, Nucl. Inst. Meth. **A352**, 573 (1995).

[2] see http://p2hp2.lanl.gov/na44/names/hubertwww/talks/talks.html under "mvd talk nov 96".

[3] see http://p2hp2.lanl.gov/na44/names/hubertwww/talks/talks.html under "gain studies, Dec 96".

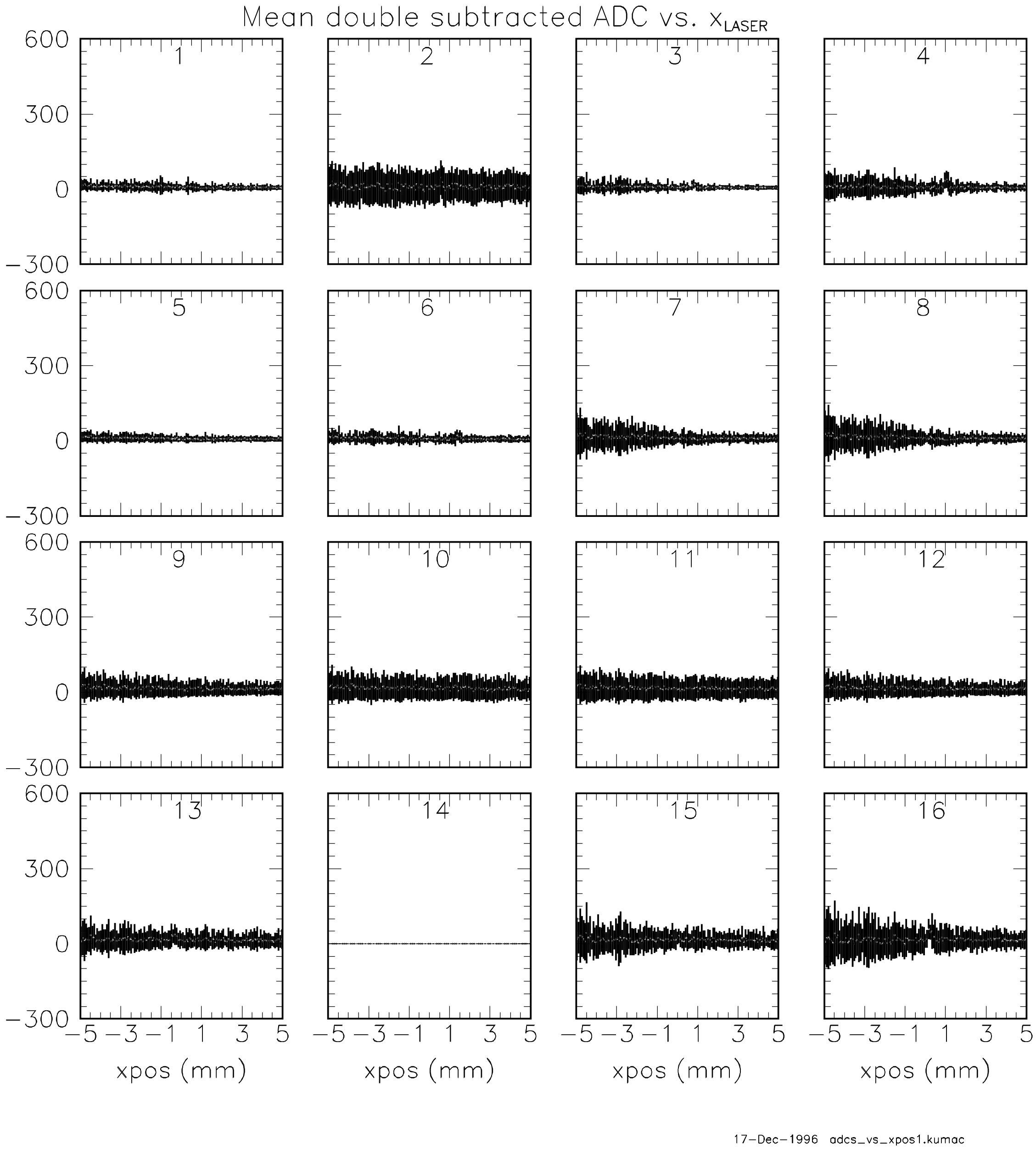

Figure 1: "Double difference" ADC distributions for channels 1-16 of the beam test electronics vs. the x position of the laser. Each bin is 80 μm wide. The definition of the origin (x=0) is arbitrary – it is the same as on the corresponding plot for channels 17-32, but different from the definition of x=0 shown in the plots for channels 33-64. The double difference is defined in the text. All measurements for channel 14 appear at ADC=0 because the pre- and post-samples were both always overflow on the ADC.

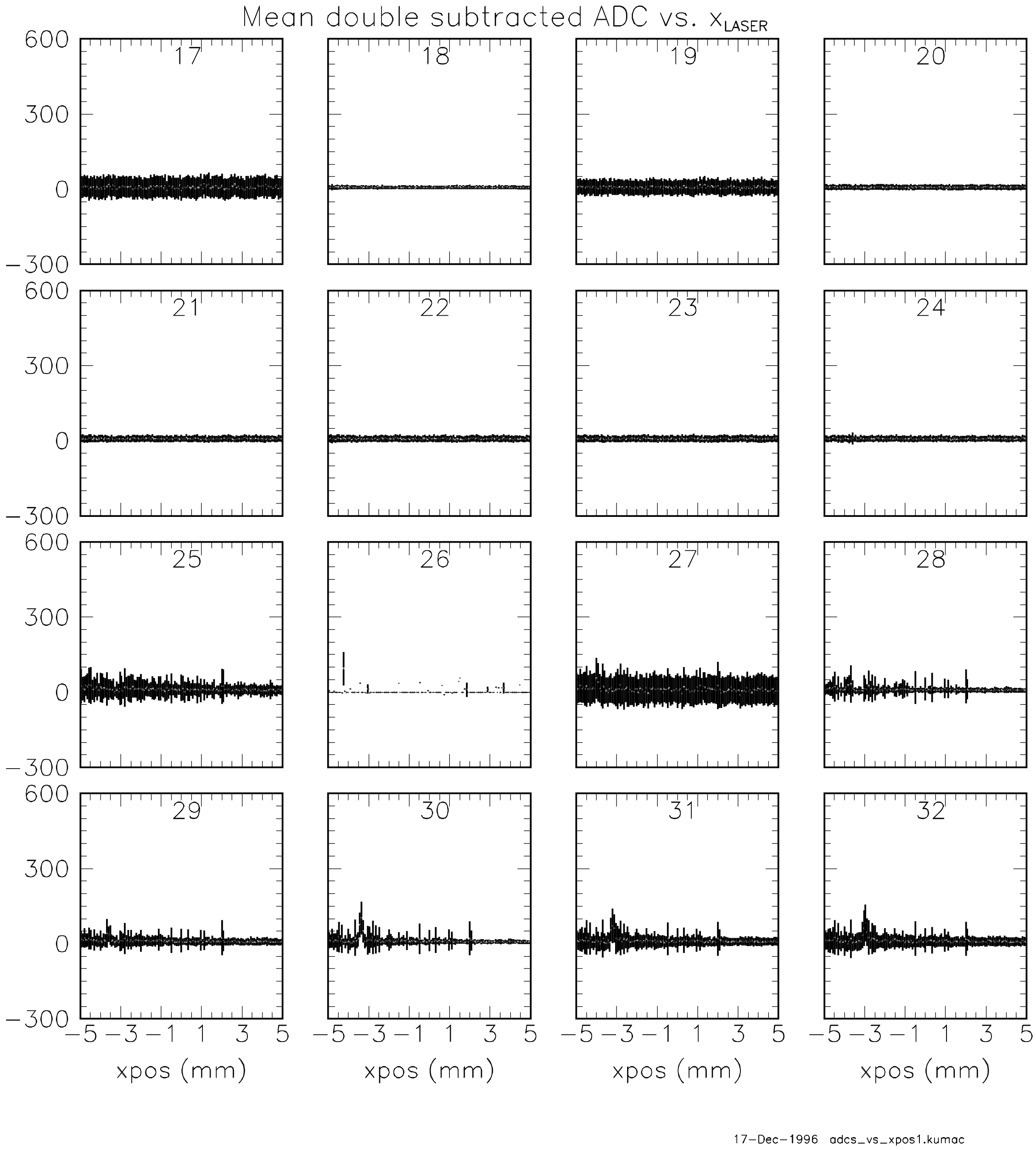

Figure 2: "Double difference" ADC distributions for channels 17-32 of the beam test electronics vs. the x position of the laser. Each bin is 80 μm wide. The definition of the origin (x=0) is arbitrary – it is the same as on the corresponding plot for channels 1-16, but different from the definition of x=0 shown in the plots for channels 33-64. The double difference is defined in the text. Almost all measurements for channel 26 appear at ADC=0 because the pre- and post-samples were both zero.

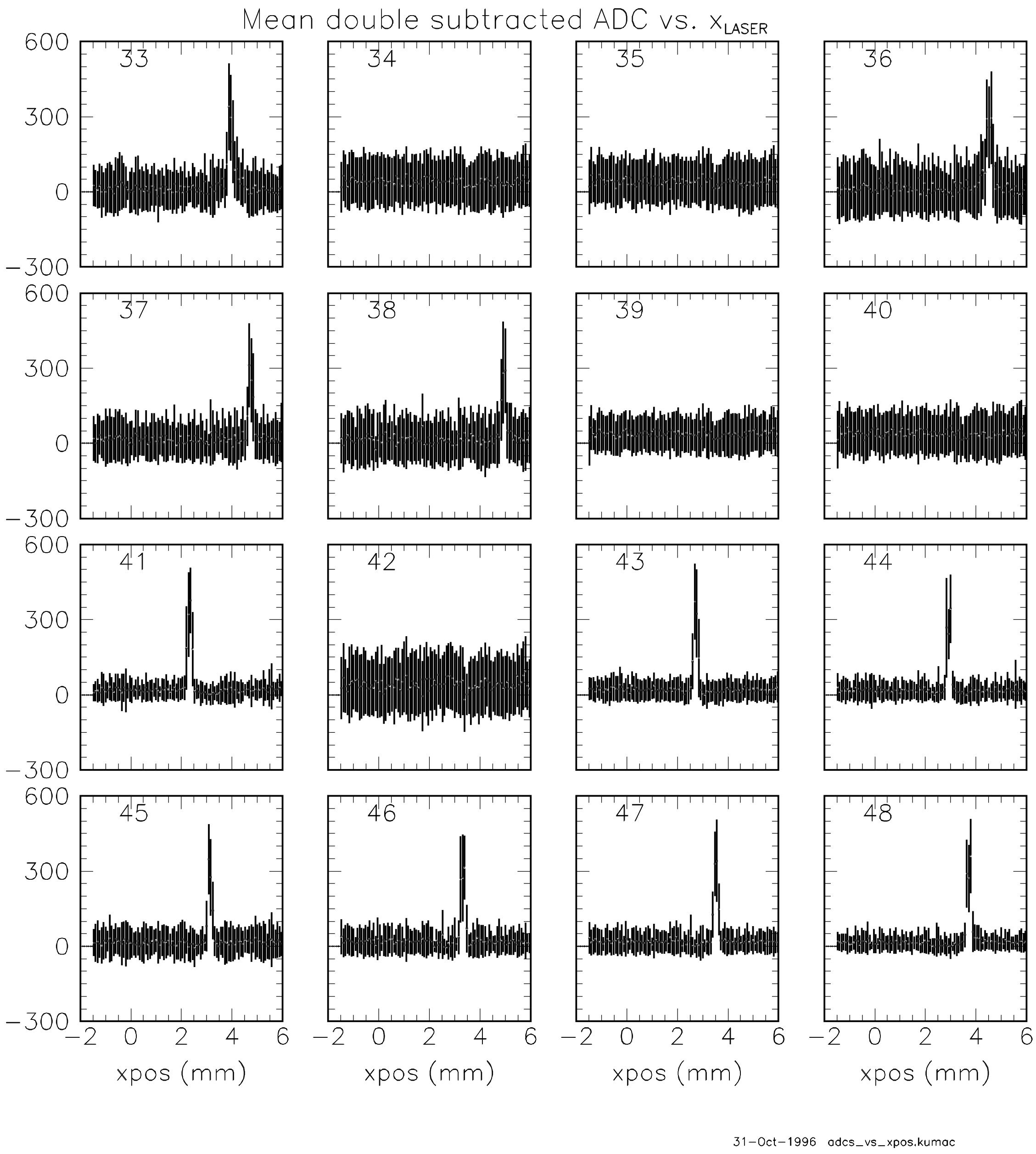

Figure 3: "Double difference" ADC distributions for channels 33-48 of the beam test electronics vs. the x position of the laser. Each bin is 80 μm wide. The definition of the origin (x=0) is arbitrary – it is the same as on the corresponding plot for channels 49-64, but different from the definition of x=0 shown in the plots for channels 1-32. The double difference is defined in the text.

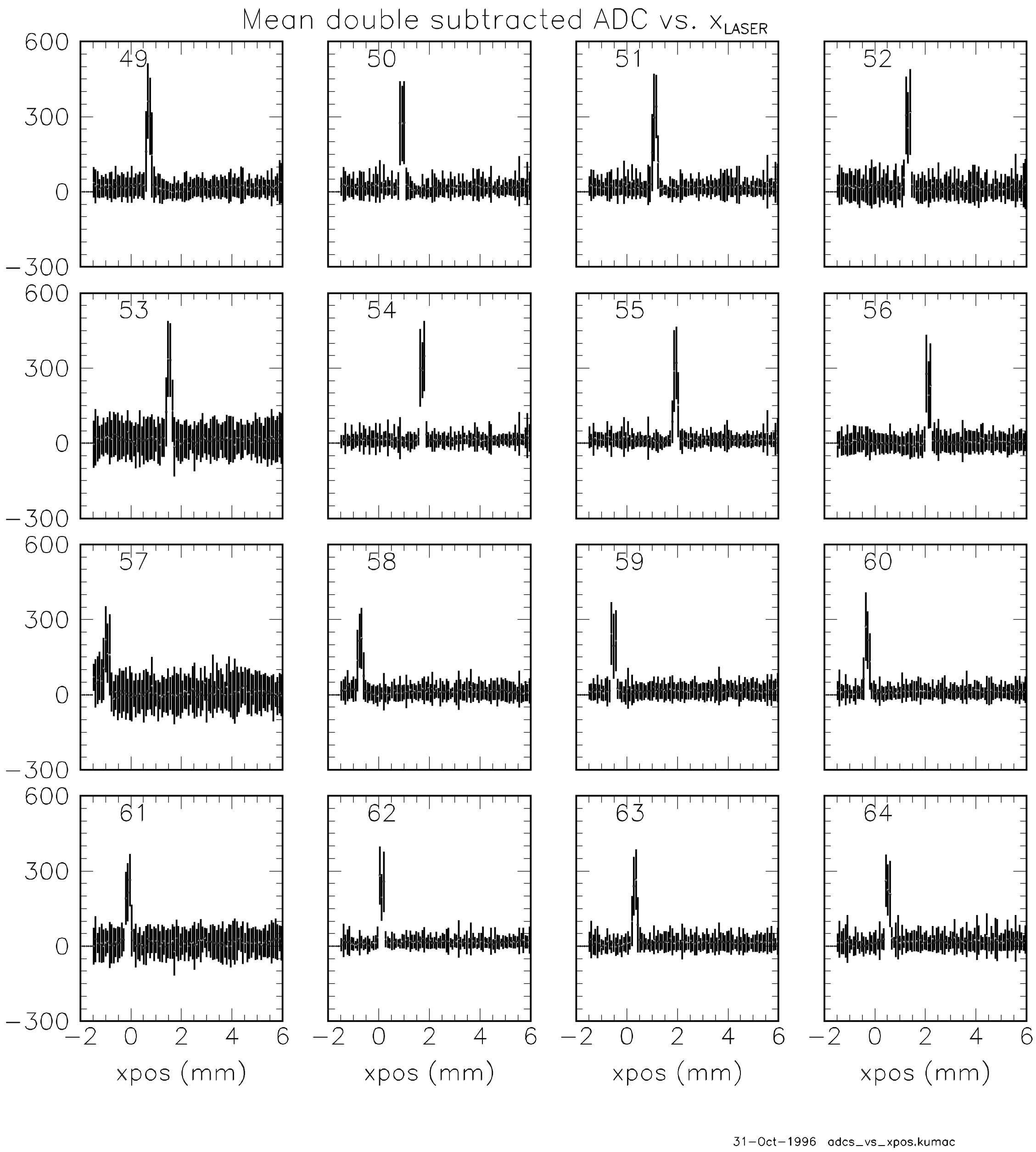

Figure 4: "Double difference" ADC distributions for channels 49-64 of the beam test electronics vs. the x position of the laser. Each bin is 80 μm wide. The definition of the origin (x=0) is arbitrary – it is the same as on the corresponding plot for channels 33-48, but different from the definition of x=0 shown in the plots for channels 1-32. The double difference is defined in the text.

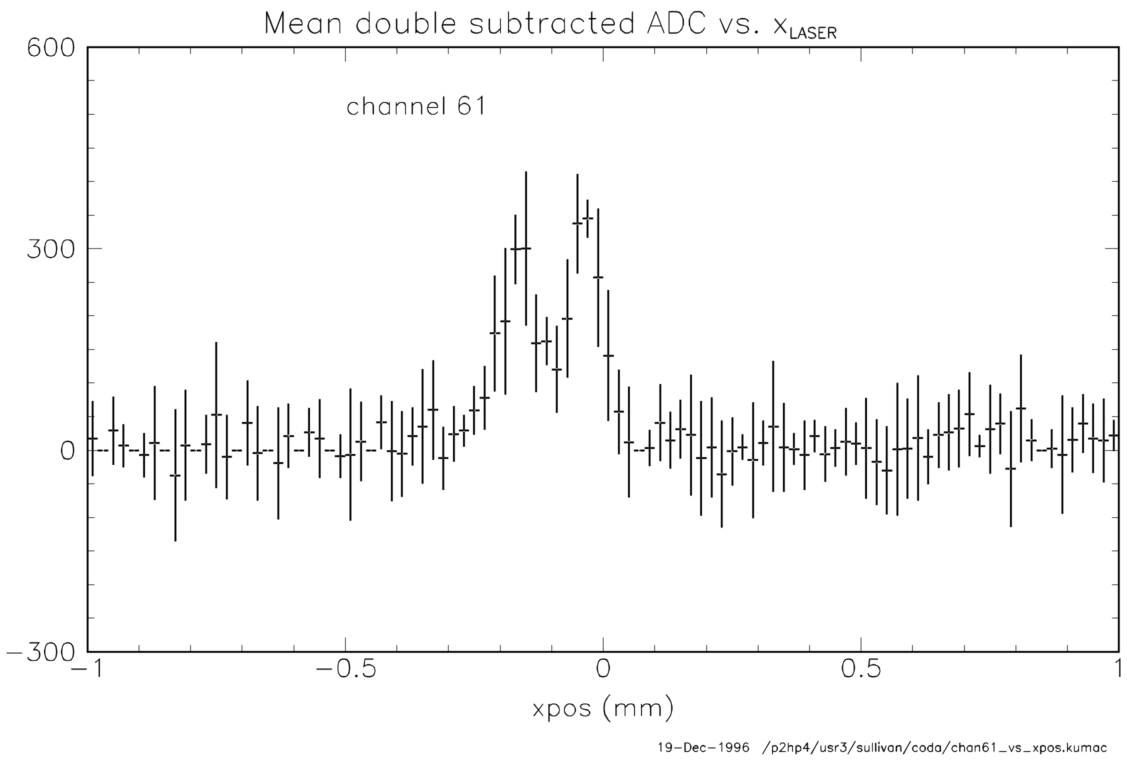

Figure 5: "Double difference" ADC distribution for channel 61 of the beam test electronics vs. the x position of the laser. Each bin is 20 μm wide. The definition of the origin (x=0) is arbitrary – it is the same as on the corresponding plots for channels 33-64, but different from the definition of x=0 shown in the plots for channels 1-32. The double difference is defined in the text.

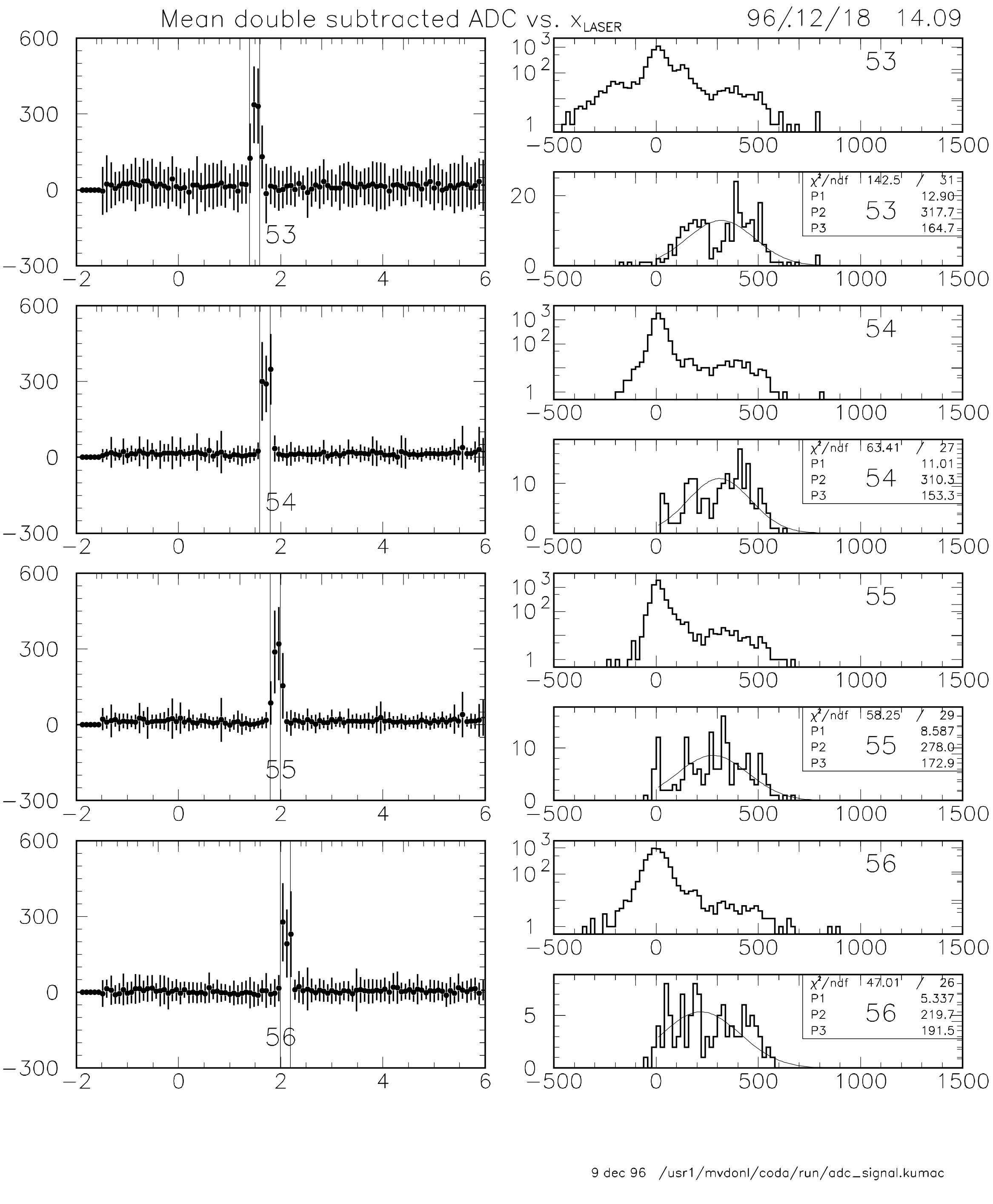

Figure 6: On the left, "Double difference" ADC distributions for channels 53-56 vs. the x position of the laser. On the right, the top plot of each pair shows the ADC distribution over the entire scan. The bottom plot of each pair shows the ADC distribution inside the narrow "signal window" marked on the left plot. The fit is a gaussian, excluding counts less than zero.

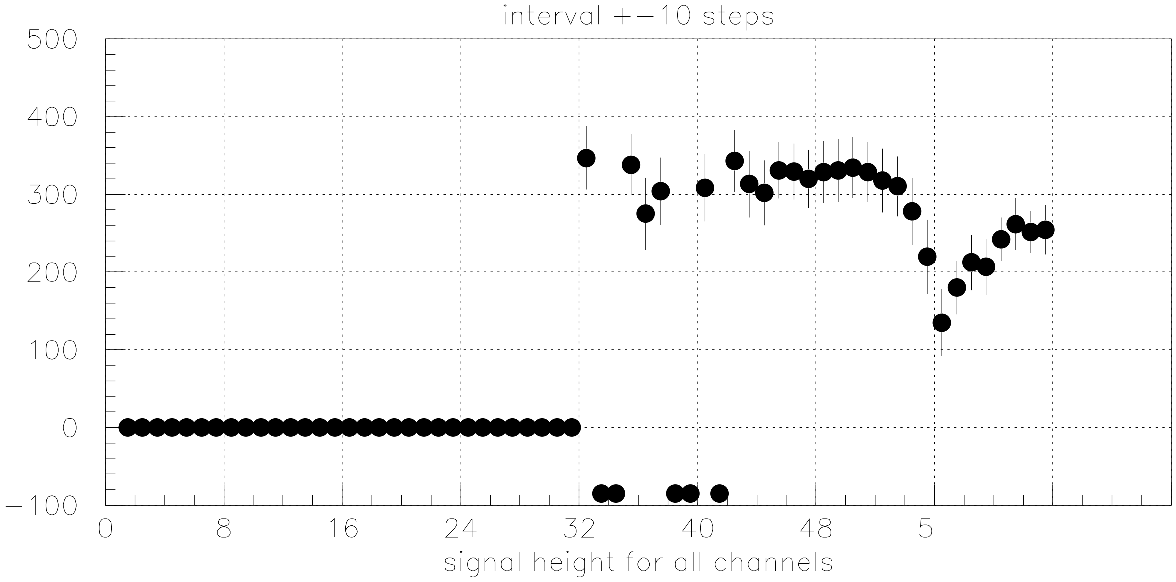

Figure 7: Summary of the relative gains for channels 33-64. Note that a "step" is 10 μm, so a window of $\pm$10 steps corresponds to $\pm$ 100 μm, or a 200 μm wide window. See the text for further details.

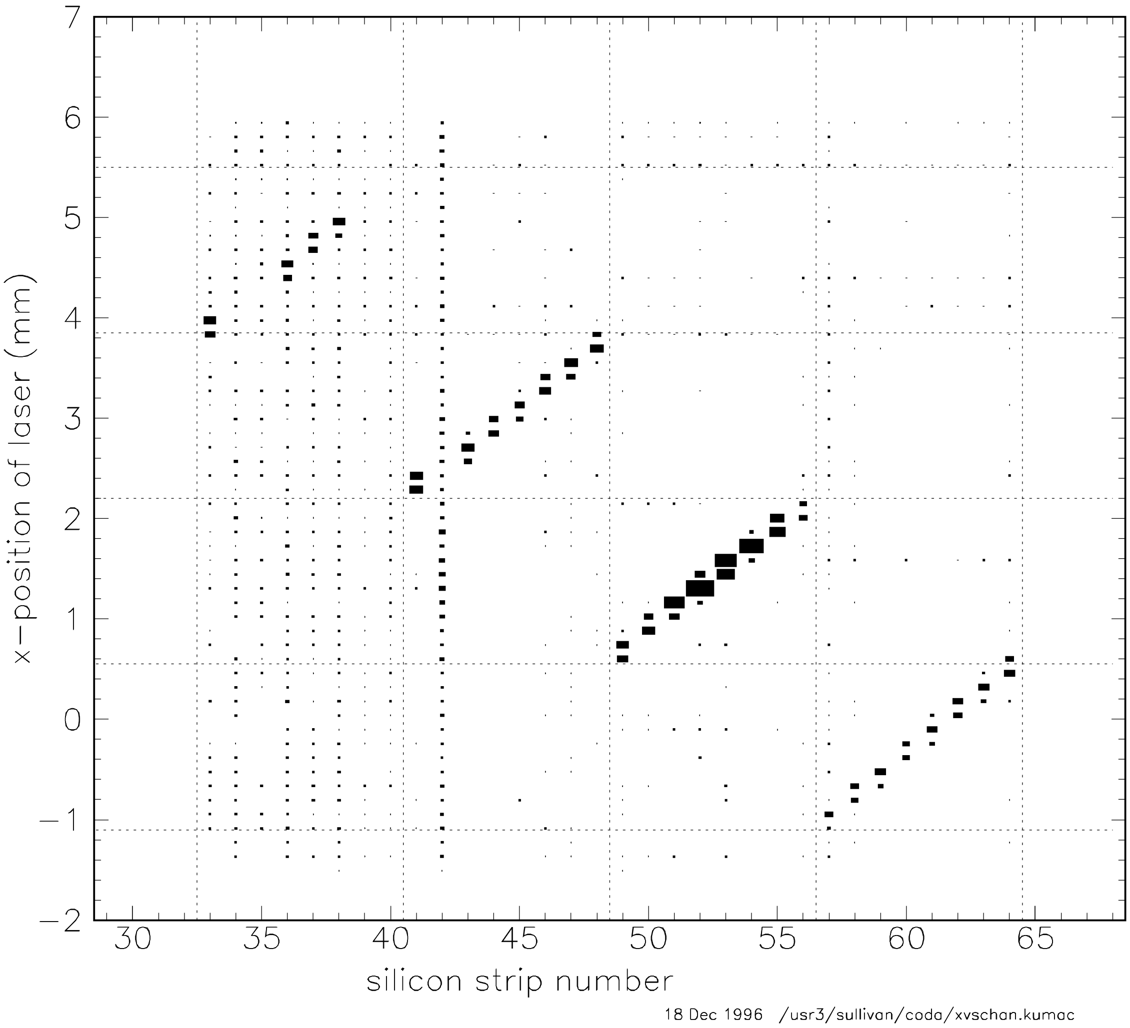

Figure 8: A 2D plot of strip number vs. the x position of the laser. The size of each box on this plot shows the number of events with the "double difference" ADC value above 200 ADC channels. The series of 4 diagonal lines represents the locations of the strips.

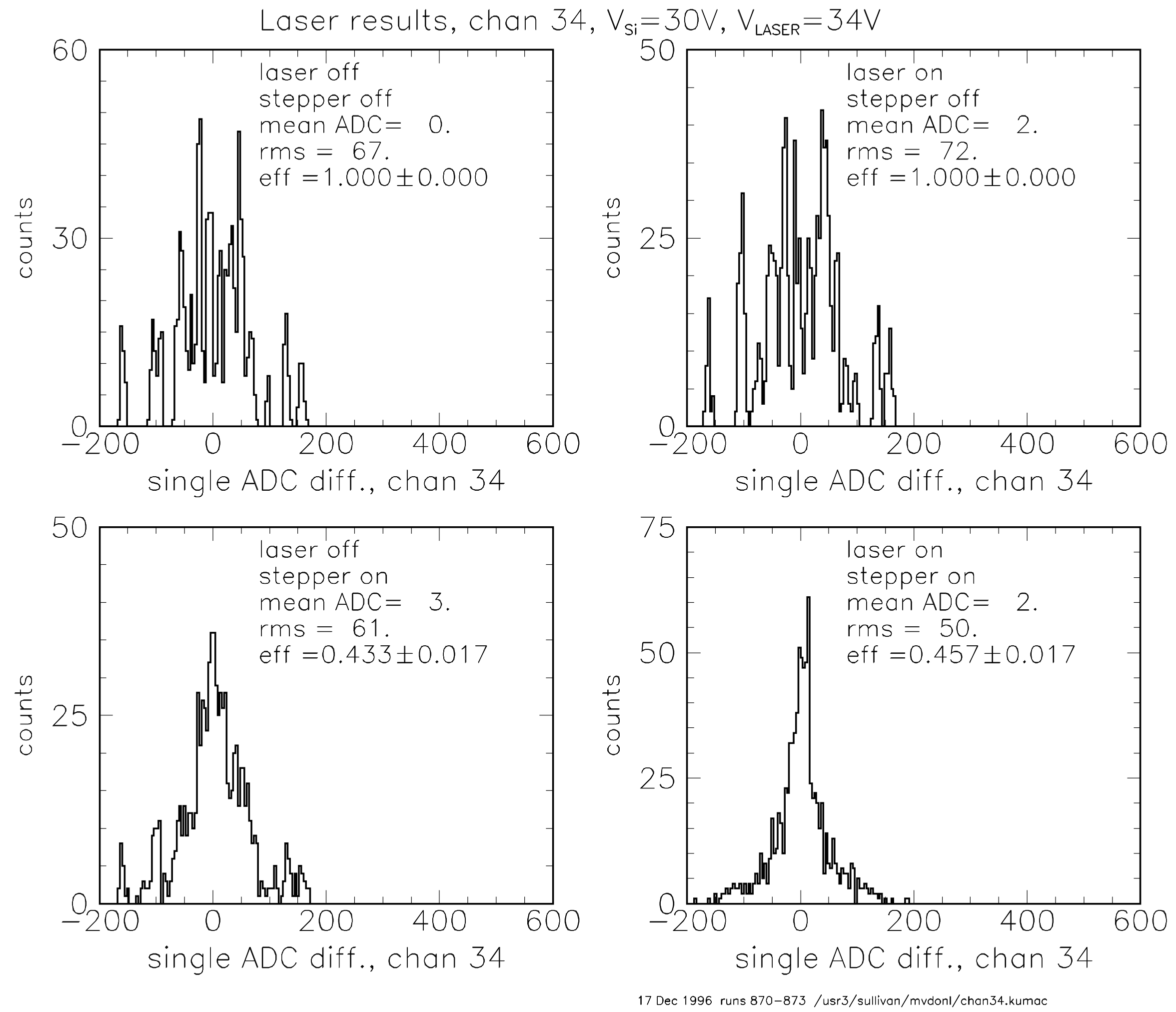

Figure 9: "Single difference" (post-sample - pre-sample) ADC distributions for chan 34, which is a channel which was **not** working in the laser station tests. The top panels show results with the stepper motor off (laser off on left, laser on shown on the right). The bottom two panels show results with the stepper motor on.

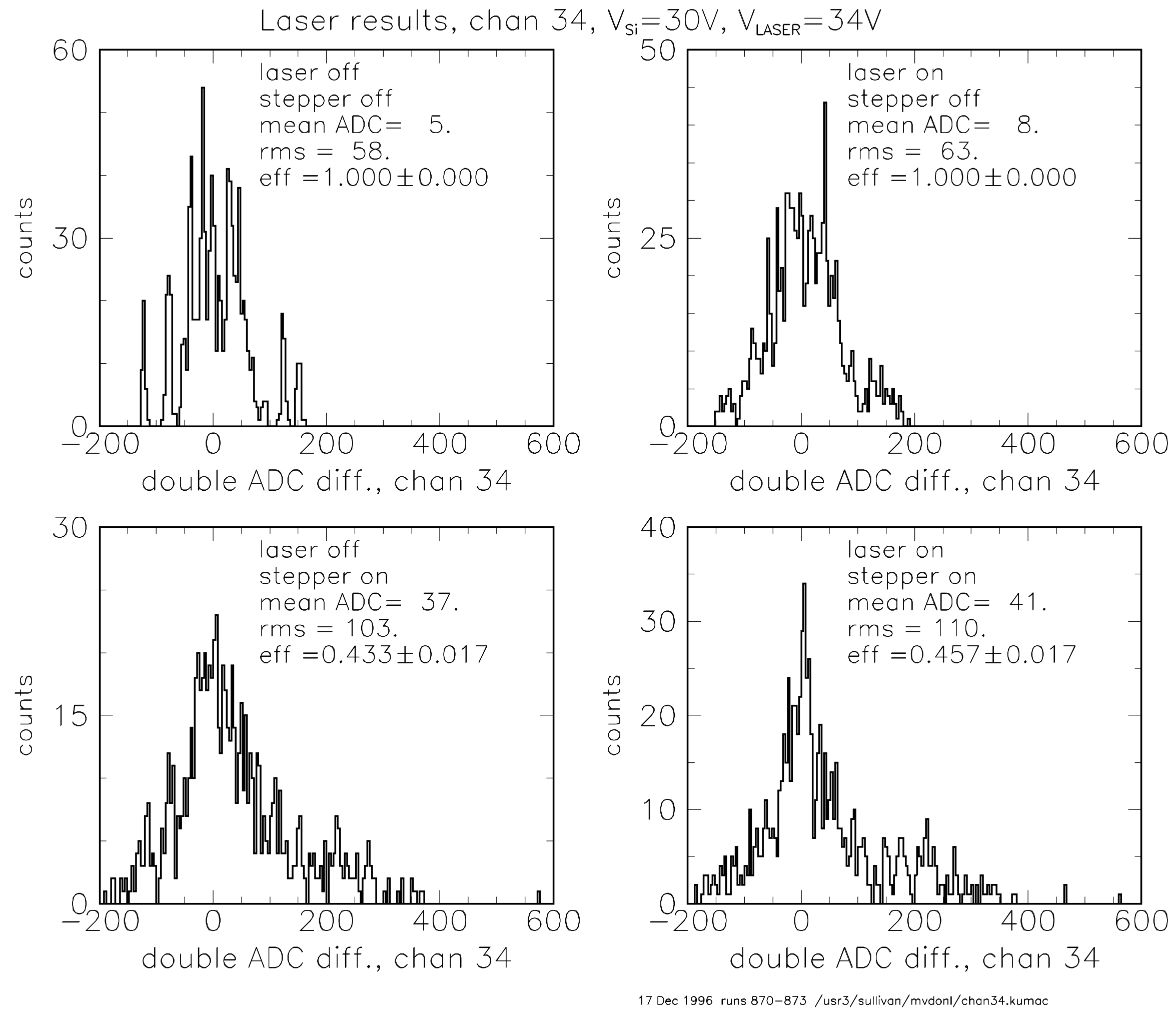

Figure 10: "Double difference" ADC distributions for chan 34, which is a channel which was **not** working in the laser station tests. The top panels show results with the stepper motor off (laser off on left, laser on shown on the right). The bottom two panels show results with the stepper motor on. See the text for the definition of the double difference.

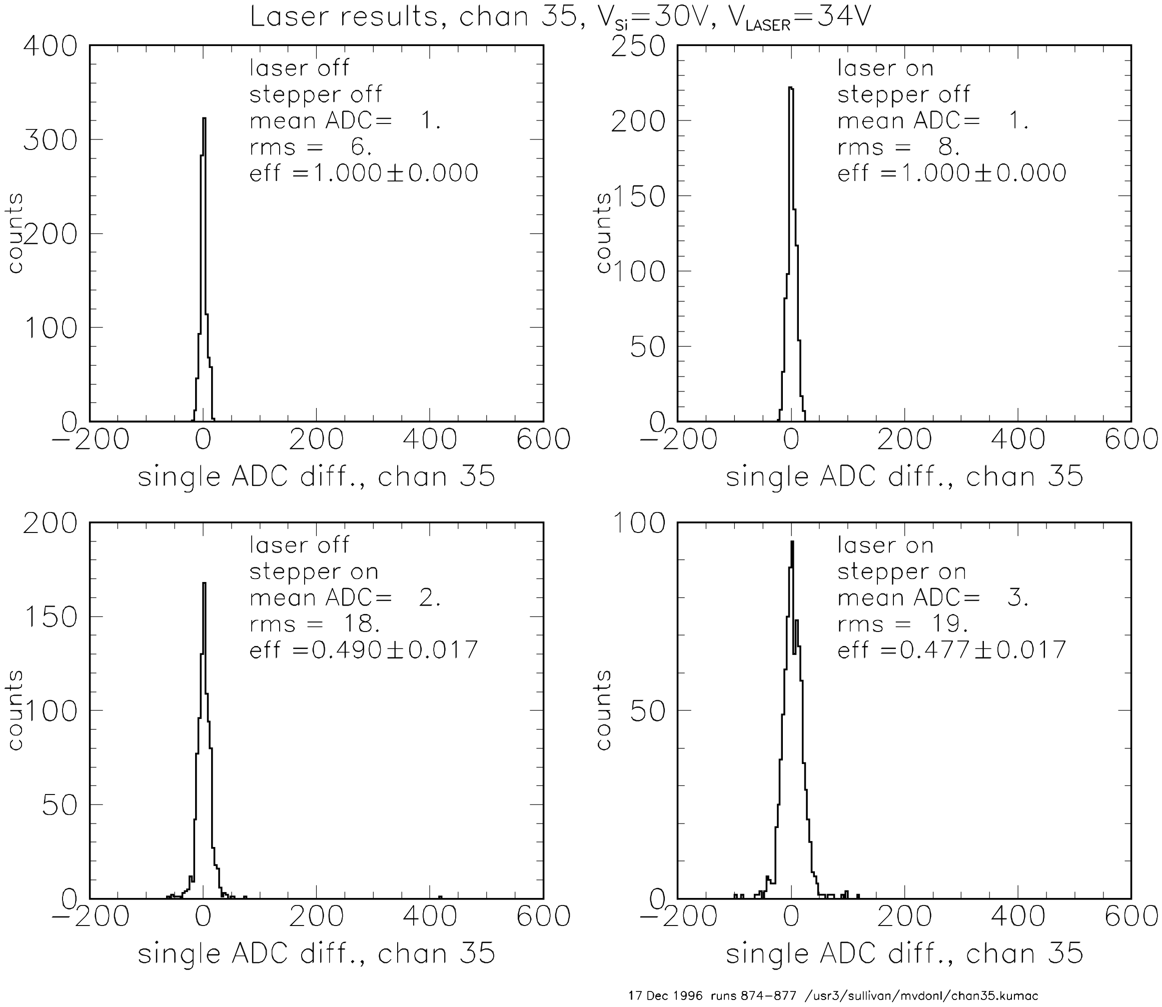

Figure 11: "Single difference" (post-sample - pre-sample) ADC distributions for chan 35, which is a channel which was **not** working in the laser station tests. The top panels show results with the stepper motor off (laser off on left, laser on shown on the right). The bottom two panels show results with the stepper motor on.

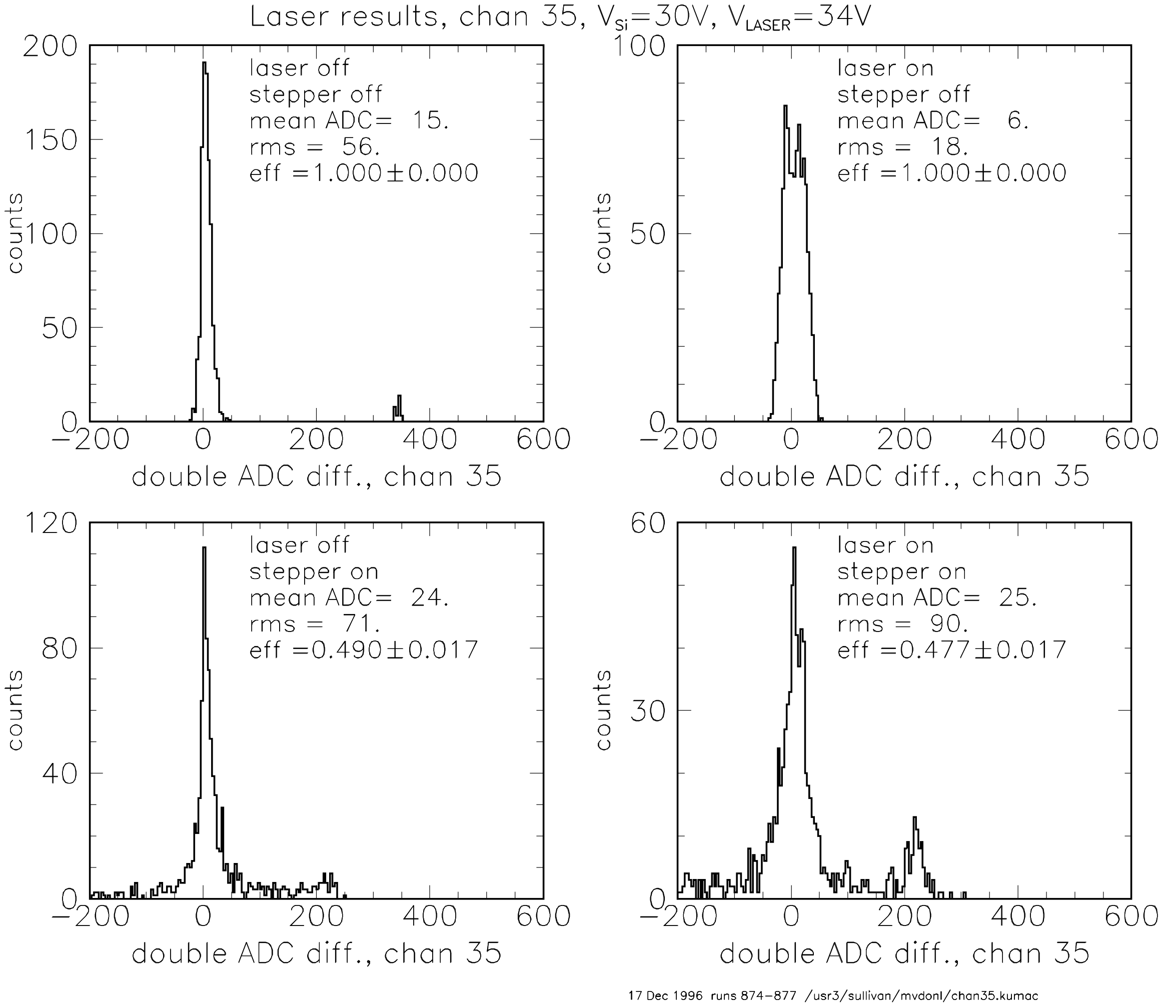

Figure 12: "Double difference" ADC distributions for chan 35, which is a channel which was **not** working in the laser station tests. The top panels show results with the stepper motor off (laser off on left, laser on shown on the right). The bottom two panels show results with the stepper motor on. See the text for the definition of the double difference.

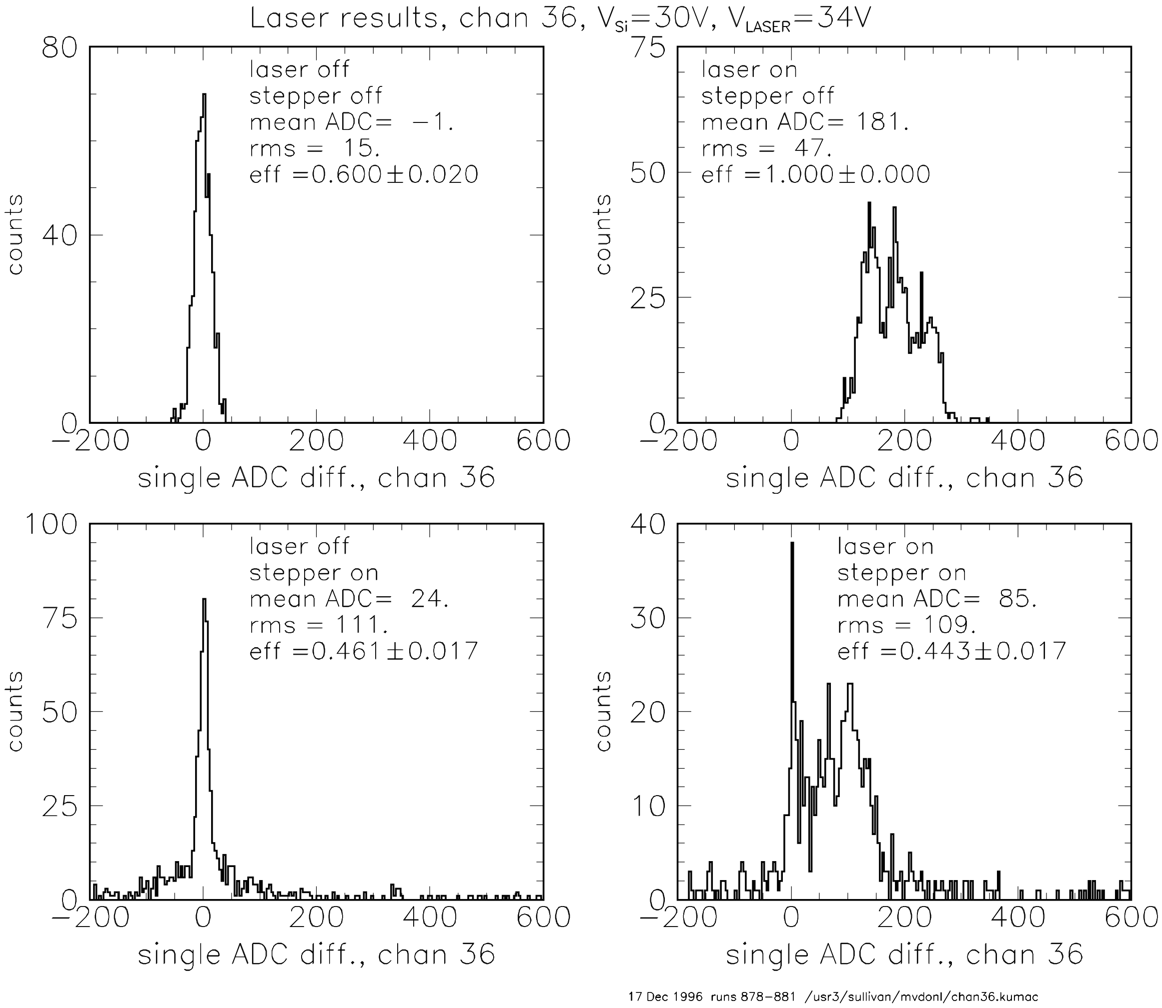

Figure 13: "Single difference" (post-sample - pre-sample) ADC distributions for chan 36, which is a channel which was working in the laser station tests. The top panels show results with the stepper motor off (laser off on left, laser on shown on the right). The bottom two panels show results with the stepper motor on.

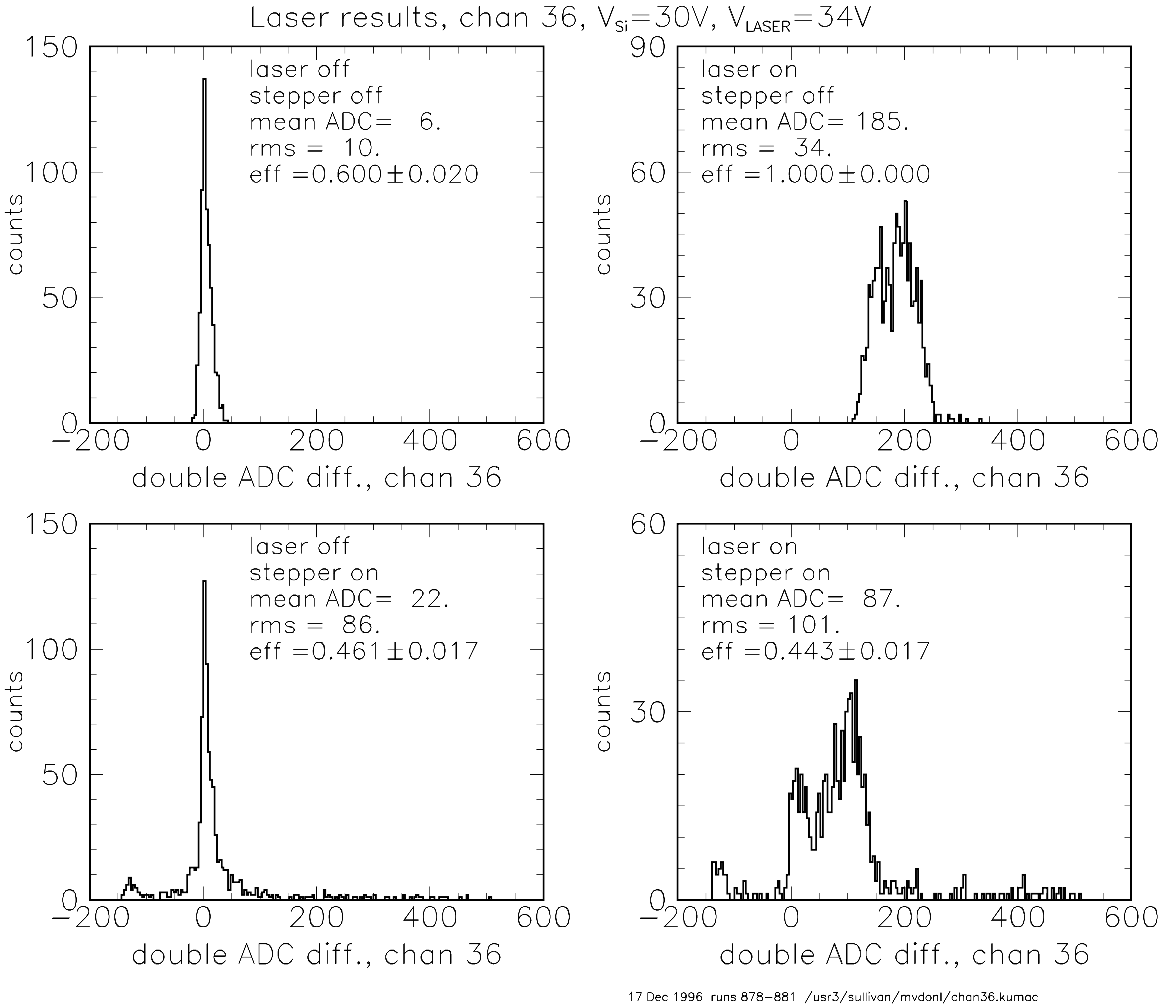

Figure 14: "Double difference" ADC distributions for chan 36, which is a channel which was working in the laser station tests. The top panels show results with the stepper motor off (laser off on left, laser on shown on the right). The bottom two panels show results with the stepper motor on. See the text for the definition of the double difference.

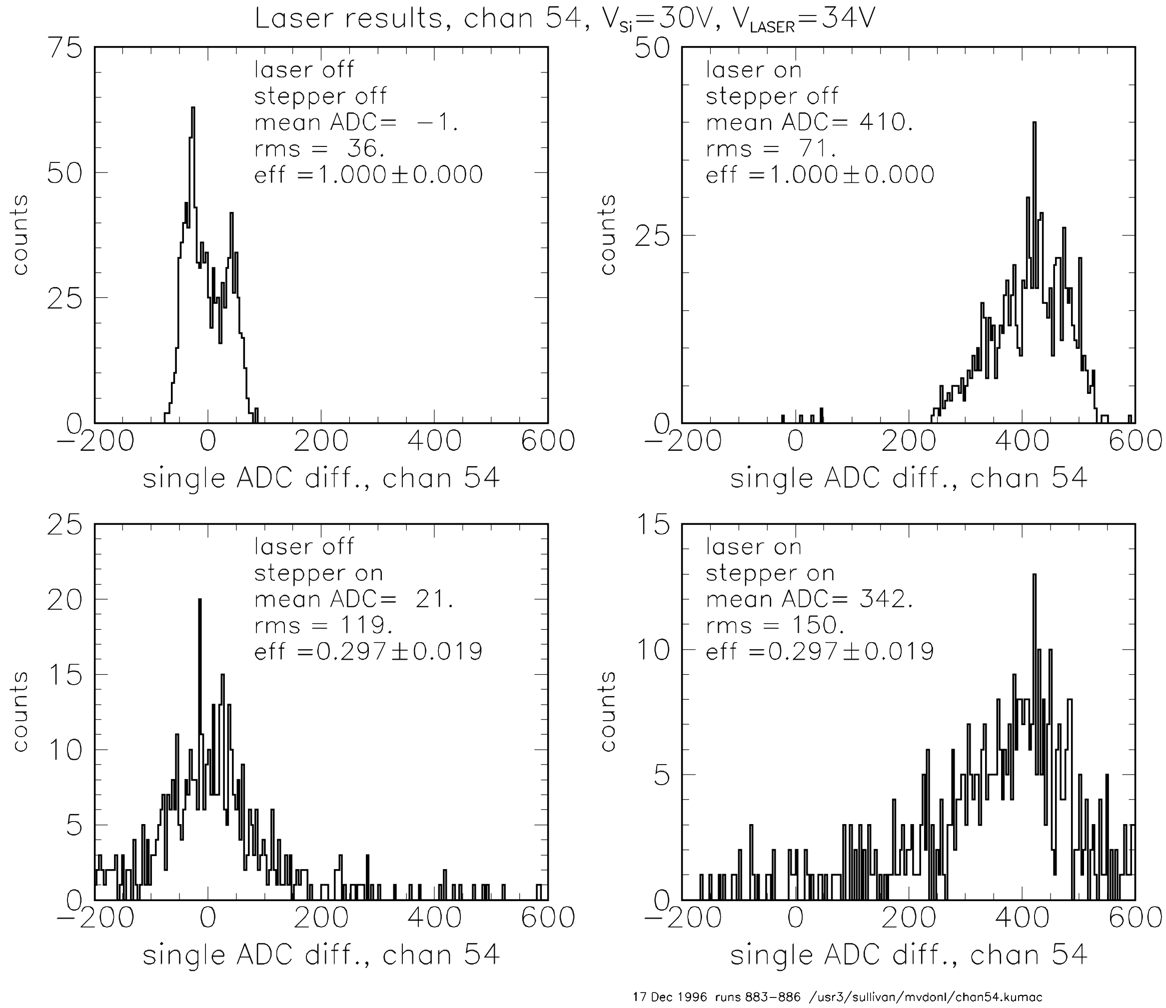

Figure 15: "Single difference" (post-sample - pre-sample) ADC distributions for chan 54, which is a channel which was working in the laser station tests. The top panels show results with the stepper motor off (laser off on left, laser on shown on the right). The bottom two panels show results with the stepper motor on. This channel was used as the "typical" channel in many of the beam test results.

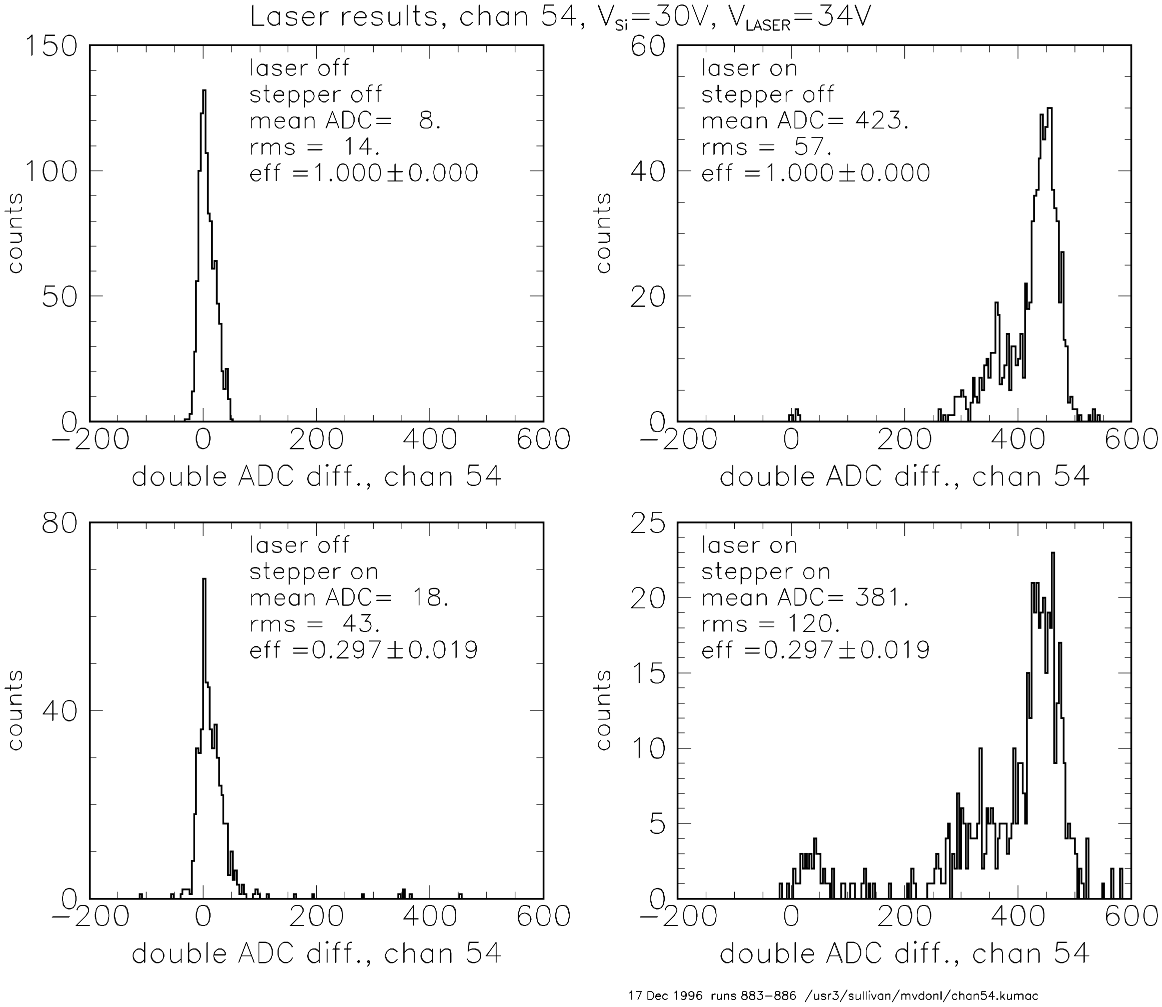

Figure 16: "Double difference" ADC distributions for chan 54, which is a channel which was working in the laser station tests. The top panels show results with the stepper motor off (laser off on left, laser on shown on the right). The bottom two panels show results with the stepper motor on. See the text for the definition of the double difference.

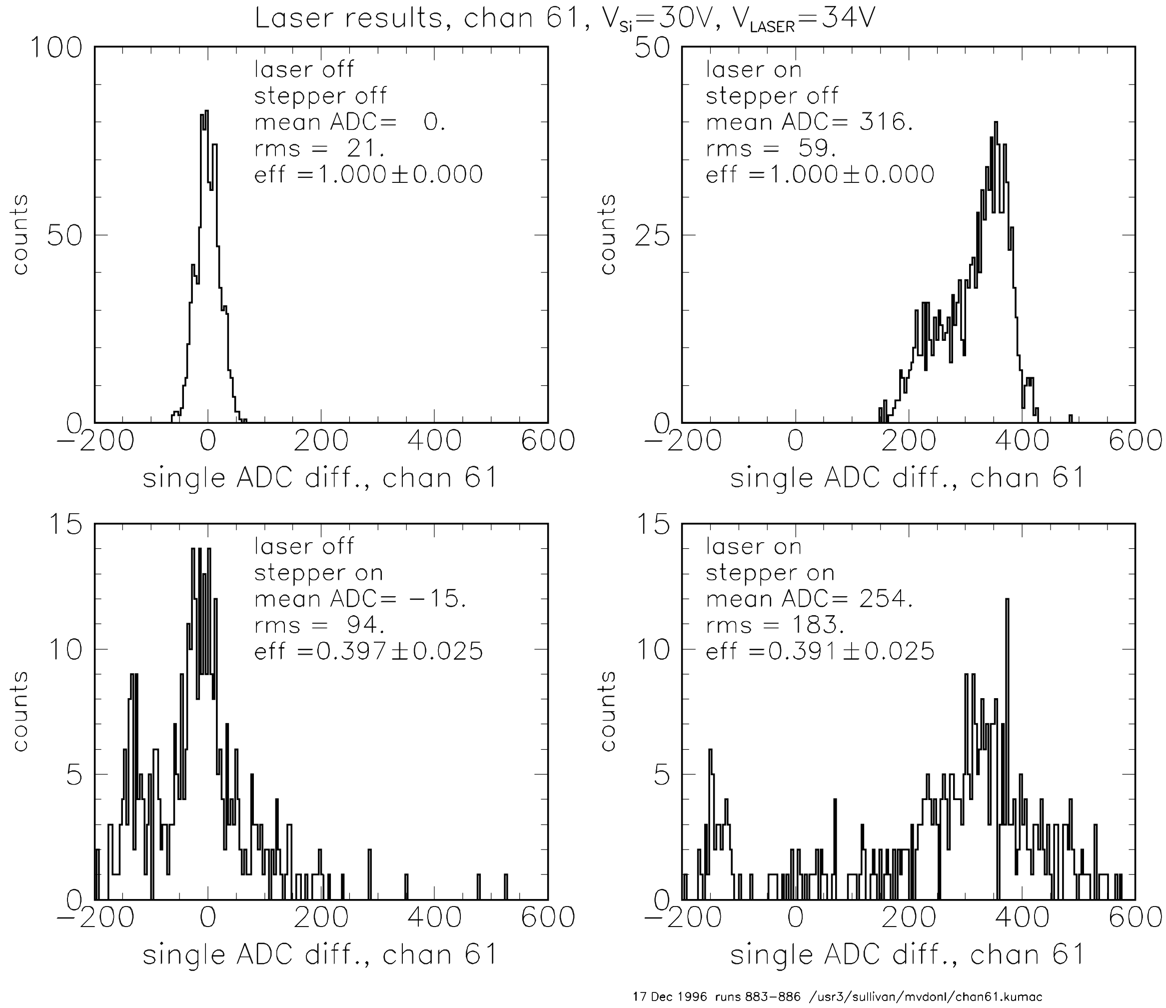

Figure 17: "Single difference" (post-sample - pre-sample) ADC distributions for chan 61, which is a channel which was working in the laser station tests. The top panels show results with the stepper motor off (laser off on left, laser on shown on the right). The bottom two panels show results with the stepper motor on.

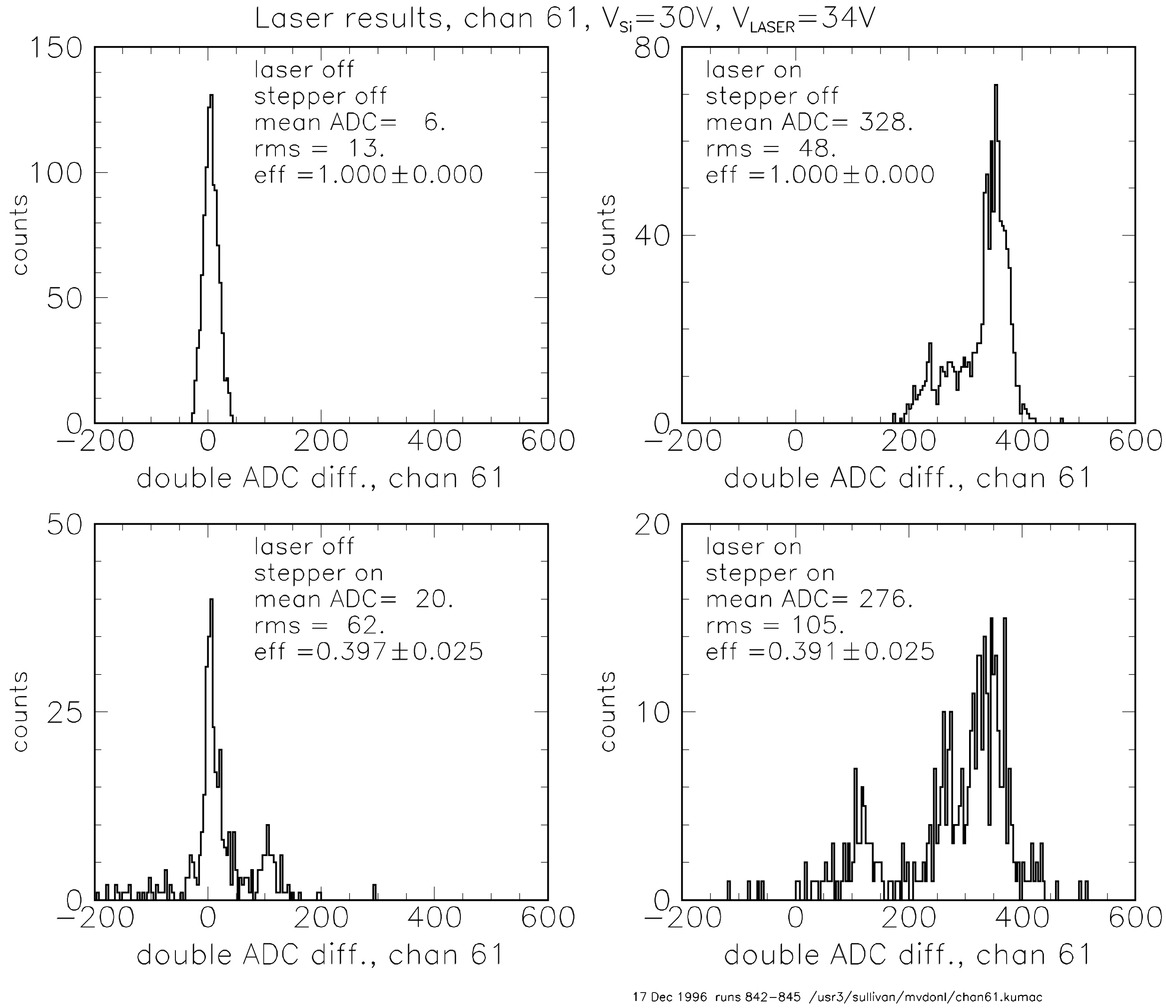

Figure 18: "Double difference" ADC distributions for chan 61, which is a channel which was working in the laser station tests. The top panels show results with the stepper motor off (laser off on left, laser on shown on the right). The bottom two panels show results with the stepper motor on. See the text for the definition of the double difference. This channel was used as the "typical" channel in many of the beam test results.